ELSEVIER

Journal of Molecular Structure (Theochem) 594 (2002) 161–172

THEO CHEM

www.elsevier.com/locate/theochem

Vitamin E models. Conformational analysis and stereochemistry of tetralin, chroman, thiochroman and selenochroman

David H. Setiadi[a,*], Gregory A. Chass[a], Ladislaus L. Torday[b], Andras Varro[b], Julius G. Papp[b,c]

[a]*Global Institute of Computational Molecular and Materials Science, VELOCET 210 Dundas Street W., Suite 810, Toronto, Ont., Canada M5G 2E8*

[b]*Department of Pharmacology and Pharmacotherapy, Szeged University, Domter12, Szeged 6701, Hungary*

[c]*Division of Cardiovascular Pharmacology, Hungarian Academy of Sciences and Szeged University, Domter12, Szeged 6701, Hungary*

Received 15 March 2002; accepted 24 April 2002

Abstract

Tetralin, chroman as well as its' S and Se containing congeners were subjected to ab initio (RHF/3-21G and RHF/6-31G(d)) and DFT (B3LYP/6-31G(d)) computation. Molecular geometries and the activation energies for ring inversions were determined with full geometry optimizations.

Keywords: Tocopherol models; Tocotrienol models; Vitamin E as an antioxidant; Molecular structure; Ring inversion; HF and DFT computations

1. Preamble

Vitamin E, a term [1] introduced in 1922, does not represent a single compound but in fact includes two families of compounds; mainly tocopherols and tocotrienols. Both families consist of a chroman (benzpyrane) ring structure and a sidechain, the latter having the characteristic isoprenoid skeleton, typical of terpenes. Members of the tocopherol family have saturated sidechains but the same sidechain in the tocotrienol family has three non-conjugated double bonds. Such carbon–carbon double bonds are separated by $-CH_2-CH_2-$ units. For both families, the carbon atom that carries the sidechain is a stereocenter of *R* configuration, however, the sidechain of the tocopherols has two additional stereocenters, at the branching points both of which are of *R* configuration. The structural variations of the two families are shown in Fig. 1.

Each of these families have four homologous members (Table 1), labeled as α, β, γ, and δ. They differ from each other in the extent of the methyl substitution in the aromatic ring. Overall, these two (2) families of compounds (tocopherol and tocotrienol) and each may come in four (4) homologous forms. The natural abundance of these $2 \times 4 = 8$ components of the vitamin E family varies from plant to plant [2] as summarized in Table 2.

* Corresponding author.

E-mail addresses: david_setiadi@hotmail.com (D.H. Setiadi), gchass@fixy.org (G.A. Chass), pyro@phcol.szote.u-szeged.hu (L.L. Torday), varro@phcol.szote.u-szeged.hu (A. Varro), papp@phcol.szote.u-szeged.hu (J.G. Papp).

0166-1280/02/$ - see front matter
PII: S0166-1280(02)00299-3

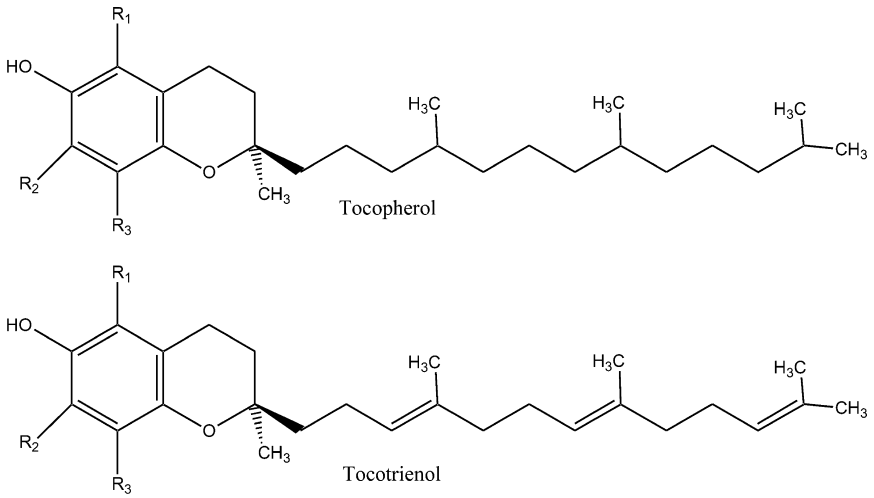

Fig. 1. Structures of tocopherols and tocotrienols. Substituents R_1, R_2 and R_3 are specified in Table 1.

Of these eight species, it is α-tocopherol which is most frequently used partly because it is commercially available in synthetic form, which does not come as a pure enantiomeric mixture. The effectiveness of the synthetic racemic mixture has traditionally been questioned, lacking an explanation at the molecular level. The primary function of vitamin E is, however, as an antioxidant, undergoing an oxidation reaction at the molecular level. Presently, we have more precise data to support this traditional assumption [3], as shown in Table 3.

Recently it has been suggested [4] that the selenium congener of α-tocopherol (Fig. 2) may be a very effective antioxidant. For this reason, we wish to study the structure of the chroman ring together with its S and Se congeners. We also wish to compare chroman with its hydrocarbon analog (tetralin).

Table 1
Extent of methyl substitutions of the tocopherol and tocotrienol families

	R_1	R_2	R_3
α	Me	Me	Me
β	Me	H	Me
γ	H	Me	Me
δ	H	H	Me

All of these compounds (**I**, **II**, **III**, and **IV**) are depicted in Section 3 below.

2. Introduction

2.1. Oxidative stress and vitamin E

One of the major current theories of aging as well as of the origin of numerous degenerative diseases is

Table 2
Typical vitamin E content of selected foods (based on α-tocopherol activity)

	Vitamin E	
	mg/100 g food portion	IU/100 g food portion[a]
Wheat germ oil	119	178
Sunflower oil	49	73
Peanut oil	19	28
Soybean oil	8.1	12
Butter	2.2	3.2
Sunflower seeds, raw	50	74
Almonds	27	41
Peanuts, dry roasted	7.4	11
Asparagus, fresh	1.8	2.7
Spinach, fresh	1.8	2.7

[a] 1 mg α-tocopherol equivalent to 1.49 IU.

Table 3
Relative activity of tocopherol and tocotrienol stereoisomers and their acetates

Natural vitamin E derivatives	Activity (%)	Synthetic vitamin E derivatives	Activity (%)
RRR-α-tocopherol	100	RRR-α-tocopheryl acetate	100
RRR-β-tocopherol	57	RRS-α-tocopheryl acetate	90
RRR-γ-tocopherol	37	RSS-α-tocopheryl acetate	73
RRR-δ-tocopherol	1.4	SSS-α-tocopheryl acetate	60
R-α-tocotrienol	30	RSR-α-tocopheryl acetate	57
R-β-tocotrienol	5	SRS-α-tocopheryl acetate	37
		SRR-α-tocopheryl acetate	31
		SSR-α-tocopheryl acetate	21

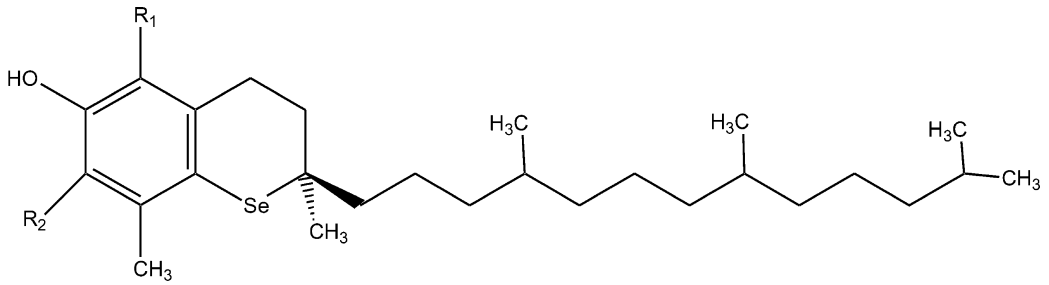

Fig. 2. Seleno-congener of α-tocopherol.

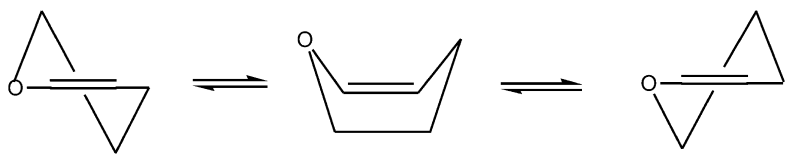

Fig. 3. Ring-flip in dihydropyran.

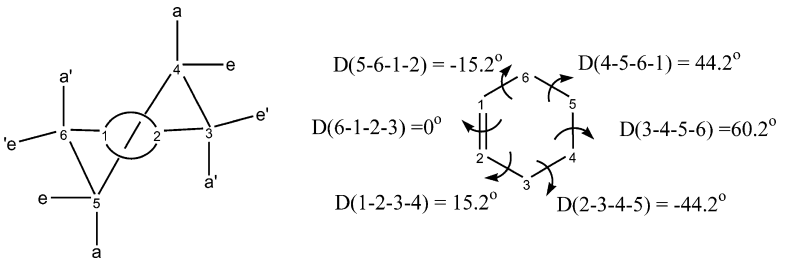

Fig. 4. Conformation and dihedral angles of cyclohexene as part of the tetralin ring system. The ring may exist in two enantiomeric forms. The signs in one of the enantiomers are as shown in the figure. In the other enantiomer, the dihedral angles are of opposite sign.

associated with a variety of free radical reactions within the human body [5]. These reactions are collectively referred to as oxidative stress.

Free radicals are generated as by-products of redox reactions associated with metabolism [6]. These include the superoxide anion (O_2^-), the hydroperoxyl radical (HOO), hydrogen peroxide (H_2O_2) and the hydroxyl radical (HO). These are collectively referred to as 'reactive oxygen species' (ROS) and are all very reactive in the body and therefore short-lived. Normally, there are natural mechanisms defending against the free radicals within the body [7], which may be enzymatic or non-enzymatic. However, if for some reason, these defense mechanisms become weakened then the free radicals can react with cellular structures such as DNA as well as proteins, or even destroy membranes through lipid peroxidation [8–10]. It is generally believed that through these processes, aging and other age-related degenerative diseases such as cardiovascular disorders and cancer are induced [1]. Recently, oxidation of a methionine residue has been implicated [11] in Alzheimer's disease as a result of oxidative stress.

Vitamin E is a potent antioxidant that helps prevent cancer by blocking lipid peroxidation, as well as the oxidation of polyunsaturated fats into free radicals. Lipid peroxidation is potentially important in all cancers but is especially significant as a cause of breast and colon cancers.

Vitamin E also serves a crucial role in the function of the immune system. A low level of this vitamin leads to impaired antibody production, inability to manufacture T and B lymphocytes and reduced resistance to cancer and infection.

Vitamin E works synergistically with vitamin C and the mineral selenium, with which it has a special affinity. Selenium and vitamin E combined, constitutes a double defense against cancer. As it is not possible to obtain optimally protective quantities of E from diet alone, supplements of 40–1600 international units (IU) are recommended daily.[1]

2.2. Structural background

One of the structural problems of vitamin E is associated with the saturated ring fused to the benzene ring. This ring cannot be considered to be cyclohexane or its heterocyclic analogues in a boat conformation because it has, at least formally, one carbon–carbon double bond. The so-called 'half-chair' conformation had been considered to be the most likely structure, before experimental observation provided strong support for that assumption.

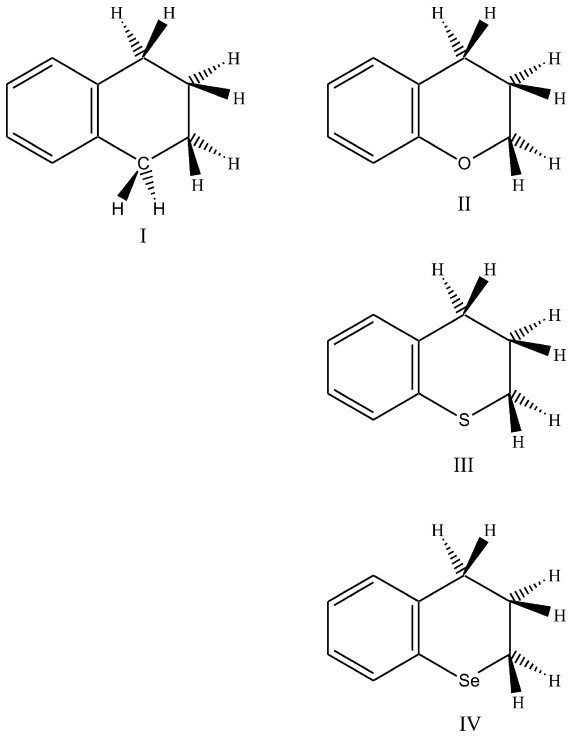

Fig. 5. Tetraline, chroman and its S and Se congeners.

The ring is expected to exist in two interconvertible enantiomeric forms, with the transition state for such a ring-flip expected to show some symmetry. It is tempting to consider the planar structure to be a good

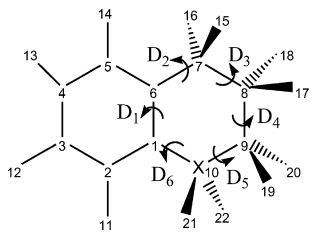

Fig. 6. Definition of the spatial orientation of atomic nuclei used for molecule including the numeric definition of relevant dihedral angles.

[1] 1 mg α-tocopherol = 1.49 IU.

Table 4
Optimized bond lengths for the stable conformers ($\lambda = 0$) of compounds **I**, **II**, **III**, and **IV** obtained at three levels of theory

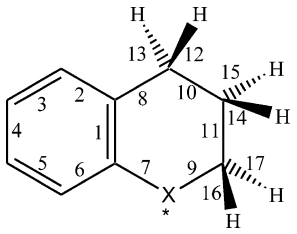

	X	1	2	3	4	5	6	7	8	9	10
HF/3-21G	CH_2	1.3900	1.3912	1.3790	1.3855	1.3790	1.3912	1.5241	1.5241	1.5374	1.5374
	O	1.3855	1.3880	1.3800	1.3872	1.3774	1.3860	1.3772	1.5197	1.4451	1.5396
	S	1.3843	1.3918	1.3787	1.3848	1.3782	1.3865	1.8356	1.5208	1.8872	1.5374
	Se	1.3862	1.3868	1.3821	1.3828	1.3814	1.3832	1.9231	1.5125	1.9950	1.5459
HF/6-31G(d)	CH_2	1.3927	1.3940	1.3799	1.3879	1.3799	1.3940	1.5191	1.5191	1.5283	1.5283
	O	1.3895	1.3923	1.3802	1.3895	1.3786	1.3906	1.3550	1.5155	1.4079	1.5283
	S	1.3924	1.3942	1.3795	1.3872	1.3786	1.3943	1.7823	1.5186	1.8133	1.5265
	Se	1.3926	1.3890	1.3843	1.3843	1.3835	1.3882	1.9073	1.5106	1.9692	1.5346
B3LYP/6-31G(d)	CH_2	1.4066	1.4026	1.3920	1.3970	1.3920	1.4027	1.5203	1.5203	1.5339	1.5338
	O	1.4054	1.4005	1.3930	1.3984	1.3908	1.4004	1.3717	1.5163	1.4306	1.5338
	S	1.4072	1.4024	1.3920	1.3965	1.3907	1.4044	1.7884	1.5182	1.8364	1.5321
	Se	1.4053	1.3996	1.3945	1.3956	1.3935	1.3998	1.9150	1.5101	1.9970	1.5421
		11	12	13	14	15	16	17	18	19	
HF/3-21G	CH_2	1.5368	1.0847	1.0871	1.0844	1.0855	1.0855	1.0844	1.0871	1.0847	
	O	1.5286	1.0836	1.0865	1.0833	1.0833	1.0837	1.0781	–	–	
	S	1.5268	1.0836	1.0870	1.0855	1.0830	1.0787	1.0791	–	–	
	Se	1.5339	1.0829	1.0865	1.0852	1.0825	1.0796	1.0791	–	–	
HF/6-31G(d)	CH_2	1.5268	1.0861	1.0889	1.0861	1.0881	1.0881	1.0861	1.0889	1.0861	
	O	1.5188	1.0853	1.0881	1.0856	1.0860	1.0878	1.0808	–	–	
	S	1.5234	1.0852	1.0887	1.0866	1.0853	1.0835	1.0828	–	–	
	Se	1.5251	1.0842	1.0886	1.0868	1.0850	1.0806	1.0804	–	–	
B3LYP/6-31G(d)	CH_2	1.5327	1.0977	1.1011	1.0968	1.0993	1.0993	1.0968	1.1010	1.0977	
	O	1.5245	1.0969	1.1002	1.0963	1.0971	1.1009	1.0932	–	–	
	S	1.5272	1.0967	1.1011	1.0977	1.0967	1.0955	1.0942	–	–	
	Se	1.5261	1.0956	1.1009	1.0982	1.0963	1.0924	1.0921	–	–	

candidate for the transition state but such a conformation could be a higher order critical point. It is more likely that the transition state is a boat conformation (Fig. 3).

Of the four CH_2 groups found in tetralin, the two allylic CH_2 exhibit quasiaxial or pseudoaxial (a') and quasiequatorial or pseudoequatorial (e') orientation, while the orientation of the central

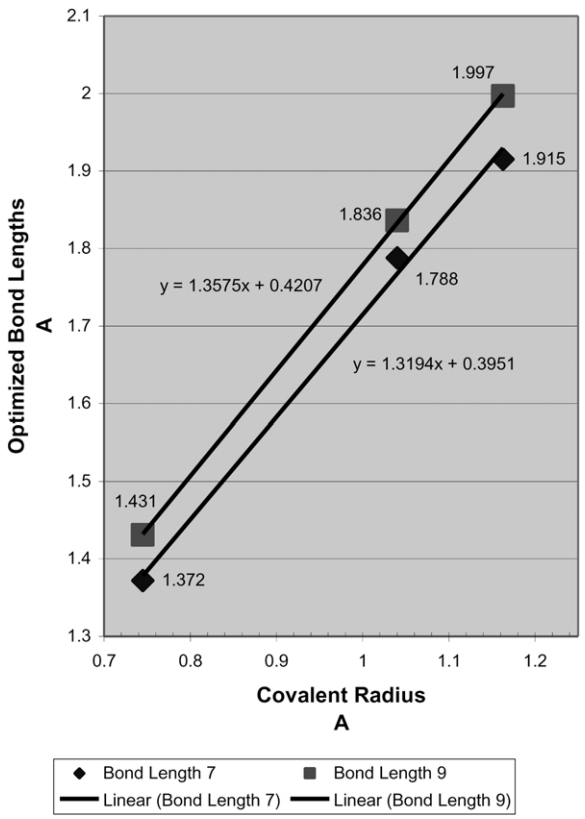

Fig. 7. Variation of selected bond lengths as a function of atomic radii.

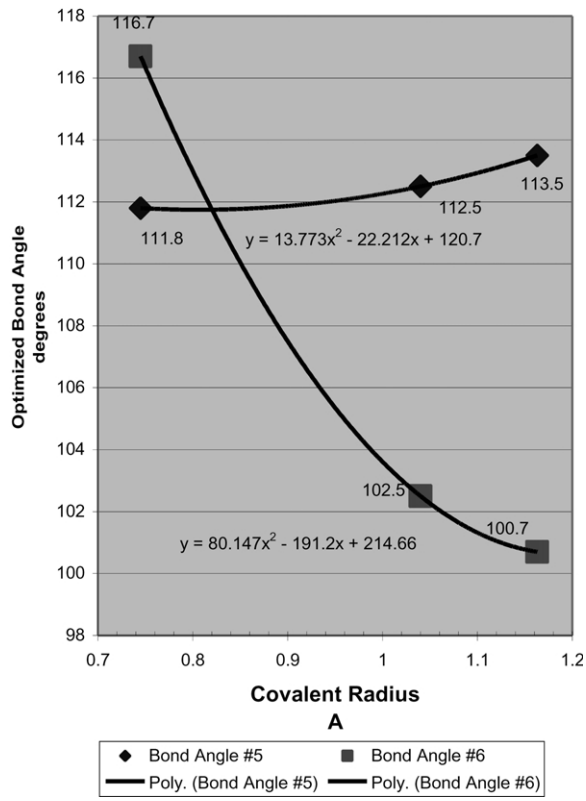

Fig. 8. Variation of selected bond-angles as a function of atomic radii.

CH_2-CH_2 moiety is expected to be close to non-cyclic molecules such as ethane or butane (Fig. 4).

Thus, the further away one moves away from the double bond, the closer one comes to the ideal planar situation. Estimated dihedral angles (D_i) are shown in Fig. 4. While we cannot extrapolate in a blindfolded way to the stereochemistry of tetralin from the conformations of cyclohexene, some analogy is nevertheless expected.

3. Method

Molecular orbital computations were carried out, using the GAUSSIAN98 program package [13], on the following four compounds: tetralin (**I**), chromane (**II**), thiochroman (**III**), and selenochroman (**IV**) as shown in Fig. 5.

Two methods and two split-valence basis sets were used, mainly the RHF/3-21G, RHF/6-31G(d) and the B3LYP/6-31G(d) levels of theory. Convergence criteria of 3.0×10^{-4}, 4.5×10^{-4}, 1.2×10^{-3}, 1.8×10^{-3} are used for the gradients of the RMS (root mean square) force, maximum force, RMS displacement and maximum displacement vectors, respectively.

Since it is generally believed that the tail end of tocopherols are only needed to enhance fat solubility [12] it is appropriate to concentrate on the fused ring systems (**II**, **III**, and **IV**). Compounds **III** and **IV** are congeners of **II**. All of these compounds lack the symmetry, which is present in **I**.

The definition of the spatial orientation of the

Table 5
Optimized bond-angles for the stable conformers ($\lambda = 0$) of compounds **I**, **II**,**III**, and **IV** obtained at three levels of theory

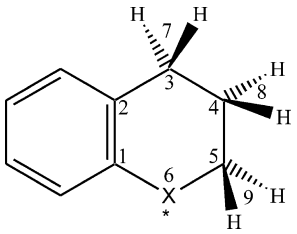

	X	1	2	3	4	5	6	7	8	9	10
HF/3-21G	CH_2	121.746	121.748	112.682	109.374	109.372	112.683	107.341	107.856	107.856	107.344
	O	122.827	120.267	110.538	108.812	110.519	118.565	106.667	108.627	109.3	–
	S	124.136	123.089	113.721	110.859	111.423	102.205	107.263	108.13	109.581	–
	Se	121.362	120.21	110.281	112.012	113.889	99.633	107.824	107.89	109.018	–
HF/6-31G(d)	CH_2	121.624	121.623	113.133	110.229	110.222	113.133	106.163	106.876	106.879	106.159
	O	122.703	120.505	110.574	109.16	111.16	117.51	106.54	107.649	108.289	–
	S	124.228	123.424	114.721	111.359	112.054	102.191	106.143	107.342	107.798	–
	Se	121.434	120.45	111.626	112.671	113.646	101.09	106.964	107.06	108.663	–
B3LYP/6-31G(d)	CH_2	121.478	121.474	113.377	110.288	110.291	113.385	105.707	106.735	106.735	105.716
	O	123.14	120.367	110.734	109.179	111.805	116.747	106.132	107.498	108.246	–
	S	124.43	123.008	114.512	111.518	112.445	102.512	105.813	107.232	107.869	–
	Se	121.524	120.5	111.714	112.709	113.499	100.694	106.843	107.001	108.92	–

Table 6
Optimized dihedral angles for the stable conformers ($\lambda = 0$) of compounds **I**, **II**, **III**, and **IV** obtained at three levels of theory

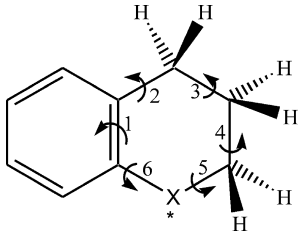

	X	1	2	3	4	5	6
HF/3-21G	CH_2	2.846	−18.423	48.888	−65.027	48.887	−18.423
	O	0.412	−20.849	49.302	−60.512	41.697	−11.236
	S	1.199	−31.5	65.183	−64.182	31.667	−1.341
	Se	−4.002	−51.068	76.461	−42.076	−4.838	29.465
HF/6-31G(d)	CH_2	2.78	−17.803	47.322	−62.972	47.335	−17.821
	O	0.557	−16.368	44.563	−61.353	47.083	−16.406
	S	2.811	−24.168	56.637	−65.581	39.916	−10.067
	Se	−3.821	−47.803	74.718	−44.392	−0.755	25.879
B3LYP/6-31G(d)	CH_2	3.264	−18.123	47.228	−62.512	47.172	−18.068
	O	0.228	−17.573	45.834	−61.223	44.939	−14.149
	S	2.654	−27.094	59.079	−64.009	36.08	−6.74
	Se	−3.888	−47.917	75.163	−44.71	−0.484	25.773

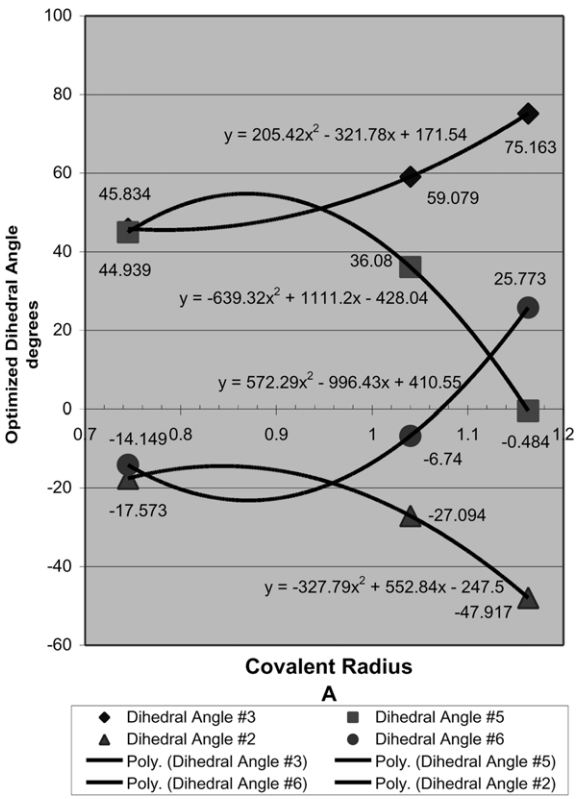

Fig. 9. Variation of selected dihedral angles as a function of atomic radii.

constituent atomic nuclei, shown in Fig. 6, was used in numerically generating the input files. No visualization tool was used for this purpose. It should be noted that H_{21} and H_{22} are present only in tetralin (**I**) but they are absent in chroman (**II**) and its higher congeners (**III** and **IV**).

For the sake of convenience, the variations of geometrical and energetic parameters from O to S to Se were fitted to quadratic functions, even though no quadratic relationships are assumed to be operative. For such graphical presentation the optimized parameters were plotted against the covalent atomic radii: O = 0.745 Å, S = 1.040 Å, and Se = 1.163 Å [14,15].

4. Results and discussion

Higher levels of theory are more reliable, therefore the majority of the discussion will be focused on the results obtained at the DFT level.

Fig. 10. RHF/6-31G(d) optimized minimum energy and transition structures for chroman. The sulphur and selenium congeners have analogous geometries.

4.1. Molecular geometry of stable structures

The optimized bond lengths show no deviations from expected structural behavior. The greatest

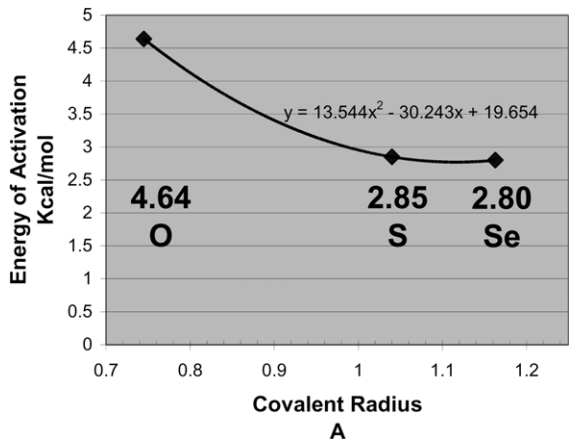

Fig. 11. Variation of energy of activation for ring inversion of chroman as well as S and Se congeners.

Table 7
Optimized bond lengths for the ring inversion transition structure ($\lambda = 1$) of compounds **I**, **II**, **III**, and **IV** obtained at three levels of theory

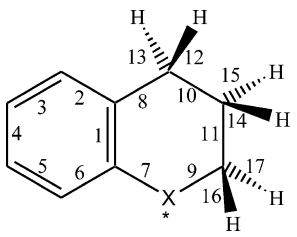

	X	1	2	3	4	5	6	7	8	9	10
HF/3-21G	CH_2	1.3909	1.3872	1.3829	1.3832	1.3830	1.3861	1.5149	1.5213	1.5406	1.5656
	O	1.3836	1.3842	1.3845	1.3848	1.3826	1.3796	1.3839	1.5153	1.4542	1.5629
	S	1.3844	1.3924	1.3794	1.3848	1.3792	1.3844	1.8296	1.5265	1.8836	1.5624
	Se	1.3852	1.3930	1.3784	1.3844	1.3780	1.3861	1.9231	1.5289	1.9724	1.5617
HF/6-31G(d)	CH_2	1.3909	1.3889	1.3847	1.3846	1.3848	1.3882	1.5113	1.5166	1.5405	1.5533
	O	1.3888	1.3855	1.3870	1.3855	1.3860	1.3821	1.3591	1.5096	1.4139	1.5454
	S	1.3930	1.3929	1.3818	1.3862	1.3811	1.3910	1.7786	1.5207	1.8135	1.5510
	Se	1.3918	1.3942	1.3811	1.3863	1.3805	1.3908	1.9063	1.5237	1.9466	1.5521
B3LYP/6-31G(d)	CH_2	1.4069	1.3996	1.3949	1.3957	1.3949	1.3988	1.5119	1.5169	1.5374	1.5602
	O	1.4021	1.3961	1.3972	1.3970	1.3960	1.3942	1.3760	1.5085	1.4388	1.5496
	S	1.4069	1.4027	1.3930	1.3965	1.3921	1.4018	1.7864	1.5208	1.8360	1.5568
	Se	1.4051	1.4040	1.3926	1.3963	1.3918	1.4006	1.9171	1.5239	1.9726	1.5580
		11	12	13	14	15	16	17	18	19	
HF/3-21G	CH_2	1.5420	1.0860	1.0834	1.0840	1.0834	1.0844	1.0839	1.0873	1.0836	
	O	1.5393	1.0848	1.0825	1.0819	1.0831	1.0775	1.0826	–	–	
	S	1.5263	1.0851	1.0831	1.0818	1.0851	1.0792	1.0788	–	–	
	Se	1.5278	1.0832	1.0854	1.0854	1.0820	1.0796	1.0807	–	–	
HF/6-31G(d)	CH_2	1.5344	1.0875	1.0847	1.0857	1.0850	1.0861	1.0864	1.0897	1.0851	
	O	1.5368	1.0866	1.0842	1.0844	1.0853	1.0802	1.0855	–	–	
	S	1.5242	1.0864	1.0842	1.0837	1.0864	1.0829	1.0831	–	–	
	Se	1.5219	1.0842	1.0865	1.0871	1.0834	1.0812	1.0817	–	–	
B3LYP/6-31G(d)	CH_2	1.5393	1.0996	1.0962	1.0968	1.0960	1.0968	1.0976	1.1017	1.0964	
	O	1.5459	1.0990	1.0953	1.0953	1.0962	1.0924	1.0984	–	–	
	S	1.5271	1.0986	1.0959	1.0950	1.0981	1.0941	1.0952	–	–	
	Se	1.5236	1.0960	1.0987	1.0990	1.0949	1.0929	1.0929	–	–	

change is expected in the C–X–C region, specifically bond lengths labeled as **7** and **9**, as shown in Table 4. The C–X involving the aromatic carbon (**7**) is slightly shorter than the other one involving the aliphatic carbon (**9**). These optimized bond lengths correlate linearly with the covalent radii of O, S, and Se, as shown in Fig. 7.

The C–X–C and the X–C–C bond-angles,

Table 8
Optimized bond-angles lengths for the ring inversion transition structure ($\lambda = 1$) of compounds **I**, **II**, **III**, and **IV** obtained at three levels of theory

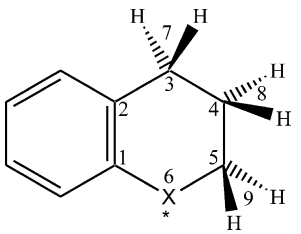

	X	1	2	3	4	5	6	7	8	9	10
HF/3-21G	CH_2	118.481	120.394	115.204	113.747	109.880	108.287	106.723	107.160	108.039	107.814
	O	119.054	118.148	113.933	112.397	111.421	112.618	107.247	107.733	109.461	–
	S	120.569	124.084	118.153	114.424	109.213	106.717	106.677	107.545	109.861	–
	Se	121.210	124.870	119.284	114.852	109.795	92.215	106.533	107.393	109.128	–
HF/6-31G(d)	CH_2	118.349	119.989	115.473	114.251	111.242	109.187	105.616	106.124	106.900	106.696
	O	118.525	116.941	112.612	112.228	112.666	112.839	106.495	106.730	108.159	–
	S	120.520	123.287	117.979	114.809	111.357	96.620	105.681	106.677	107.989	–
	Se	120.409	124.462	119.366	115.423	109.822	93.170	105.539	106.754	108.826	–
B3LYP/6-31G(d)	CH_2	118.318	119.932	115.608	114.075	111.247	109.269	105.202	106.025	106.843	106.432
	O	118.847	116.619	112.609	112.047	113.735	112.492	106.344	106.758	108.125	–
	S	120.632	123.246	118.153	114.607	111.553	96.357	105.249	106.592	108.111	–
	Se	120.556	124.466	119.483	115.213	109.884	92.727	105.130	106.676	109.050	–

labeled **6** and **5**, respectively, are of greatest interest. The results are summarized in Table 5. Values show bond-angle **6** as undergoing the greatest change as the bond-angle (**6**) moves from a value larger than tetrahedral towards 90°, typical of S and Se. The diminishing of the C–C–C bond-angle is nearly exponential. In contrast to this, the X–C–C bond-angle (**5**) is compensating for such a dramatic closing in **6**, through a modest opening in the X–C–C (**5**) values. These changes at the DFT level are evaluated as moving from 111.8° for (X = oxygen) to 113.5° (X = selenium). The change is illustrated in Fig. 8.

For the torsion of the heterocyclic ring, dihedral angles behave in an interesting way as summarized in Table 6. The dihedral angles **1** and **4** behave in non-routine fashion, much as if the influence of the X nucleus on these two dihedrals was inconsequential. Dihedral angles **2** and **6** are similar in magnitude and **3** and **5** are nearly identical. Yet they show deviation from one another as X = oxygen is replaced by sulfur and then by selenium. The variations of these dihedral angles are shown in Fig. 9.

4.2. Molecular geometries at transition structures

The ring inversion (Fig. 3) was studied in the cases of compounds **I**, **II**, **III**, and **IV**. For compound **II** (X = oxygen) the initial state, the transition state and the final states are shown in Fig. 10 as structures optimized at the RHF/6-31G(d) level of theory. Clearly, the fused heterocyclic ring exhibits a highly distorted boat arrangement (Fig. 10) in comparison to the idealized case given in Fig. 3. The optimized geometrical parameters, specifically bond lengths, bond-angles,

Table 9
Optimized dihedral angles lengths for the ring inversion transition structure ($\lambda = 1$) of compounds **I**, **II**, **III**, and **IV** obtained at three levels of theory

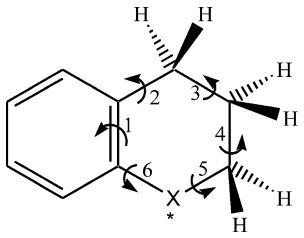

	X	1	2	3	4	5	6
HF/3-21G	CH_2	−5.450	29.194	−3.496	−41.810	64.682	−41.565
	O	−6.334	34.135	−12.900	−32.037	62.593	−43.335
	S	−5.213	26.268	8.548	−56.141	65.340	−36.158
	Se	5.727	−25.247	−10.899	57.659	−63.418	33.606
HF/6-31G(d)	CH_2	−5.373	30.931	−7.783	−37.100	61.774	−40.922
	O	−4.317	38.477	−22.512	−23.716	60.899	47.071
	S	−5.557	27.952	3.567	−51.108	63.113	−35.800
	Se	5.702	−26.868	−8.217	55.624	−63.275	34.382
B3LYP/6-31G(d)	CH_2	−5.942	30.989	−7.284	−37.662	61.906	−40.379
	O	−4.454	41.093	−27.214	−19.083	57.513	−46.097
	S	−7.029	28.945	3.624	−51.440	62.871	−34.495
	Se	6.923	−27.559	−8.676	56.325	−62.266	33.300

and dihedral angles are summarized in Tables 7–9, respectively.

4.3. Energetics of ring inversion

The energies of activations for the four compounds are tabulated in Table 10 at three levels of theory. The E_a values for the X = [O,S,Se] containing molecules (**II**, **III**, and **IV**, respectively) were plotted against the covalent radii of X. The difference between O and S is large while the difference between S and Se is small (Fig. 11).

5. Conclusions

It is in human nature to wonder if 'Mother Nature' did the best possible structural arrangement or whether we can improve upon it. The question has been asked [13,14] in general, about antioxidants and in particular about vitamin E [16,17].

From the present study, one can see that the influence of X = S (**III**) and X = Se (**IV**) are analogous to one another other but that they are very much different from the X = O congener (**II**). On the basis of this result, one may expect the sulfur and the selenium containing compounds to be either much weaker or much stronger antioxidants than the oxygen containing one. Further research is needed in this area, in order to quantify the antioxidant characteristics of all topologically probable conformers, for each of these molecular systems.

Table 10
Optimized total energies for stable conformers ($\lambda = 0$) and ring inversion transition structure ($\lambda = 1$) as well as the associated energy of activation of compounds **I**, **II**, **III**, and **IV** obtained at three levels of theory

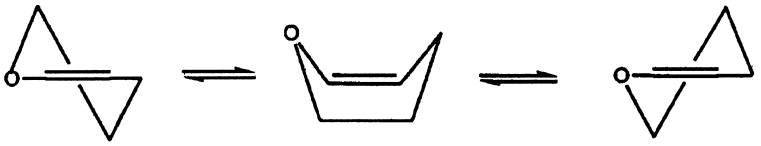

	E (hartree)		
X	Min	TS	E_a (kcal/mol)
HF/3-21G			
CH_2	−383.543851545	−383.538891934	3.112205499
O	−419.162508351	−419.154678402	4.913371297
S	−740.280616962	−740.276189519	2.778264757
Se	−2733.219289040	−2733.212773800	4.088378253
HF/6-31G(d)			
CH_2	−385.686372822	−385.680849545	3.465911550
O	−421.501191382	−421.493978702	4.526028827
S	−744.156982123	−744.152313980	2.929306414
Se	−2744.222591050	−2744.218050310	2.849359758
B3LYP/6-31G(d)			
CH_2	−388.306393922	−388.301776427	2.897524287
O	−424.203406366	−424.196005393	4.644184567
S	−747.177884971	−747.173343996	2.849507222
Se	−2748.368331440	−2748.363874870	2.796542241

References

[1] M. Evans, K.S. Bishop, Science 55 (1922) 650.
[2] J.B. Bauernfeind, Vitamin E: A Comprehensive Treatise, Marcel Dekker, New York, 1980, pp. 99–167.
[3] B. Weimann, H. Weiser, Am. Clin. Nutr. 53 (1991) 1056S–1060S.
[4] N. Al-Maharik, L. Engman, J. Malmstrom, C. Schiesser, Intramolecular homolytic substitution at selenium: synthesis of novel selenium-containing vitamin E analogues, J. Org. Chem. 66 (2001) 6286–6290.
[5] A.D.N.G. de Grey, The Mitochondrial Free Radical Theory of Aging, R.G. Landes Company, Austin, TX, 1999.
[6] B. Chance, H. Sies, A. Boveris, Physiol. Rev. 59 (1979) 527.
[7] B.N. Ames, M.K. Shigenaga, in: J.G. Scandalios (Ed.), Molecular Biology of Free Radical Scavenging Systems, Cold Spring Harbor Laboratory Press, New York, 1992, p. 1.
[8] S. Steenken, Chem. Rev. 89 (1979) 503.
[9] K.L. Fong, P.B. McCay, J.L. Poyer, B.H. Misra, B. Keele, J. Biol. Chem. 248 (1973) 7792.
[10] T.I. Mak, W.B. Weglicki, J. Clin. Invest. 75 (1985) 58.
[11] S. Varadarajan, J. Kanski, M. Aksenova, C. Lauderback, D.A. Butterfield, J. Am. Chem. Soc. 123 (2001) 5625.
[12] G.W. Burton, K.U. Ingold, Acc. Chem. Res. 19 (1986) 194.
[13] M.J. Frisch, G.W. Trucks, H.B. Schlegel, G.E. Scuseria, M.A. Robb, J.R. Cheeseman, V.G. Zakrzewski, J.A. Montgomery Jr., R.E. Stratmann, J.C. Burant, S. Dapprich, J.M. Millam, A.D. Daniels, K.N. Kudin, M.C. Strain, Ö. Farkas, J. Tomasi, V. Barone, M. Cossi, R. Cammi, B. Mennucci, C. Pomelli, C. Adamo, S. Clifford, J. Ochterski, G.A. Petersson, P.Y. Ayala, Q. Cui, K. Morokuma, D.K. Malick, A.D. Rabuck, K. Raghavachari, J.B. Foresman, J. Cioslowski, J.V. Ortiz, A.G. Baboul, B.B. Stefanov, G. Liu, A. Liashenko, P. Piskorz, I. Komaromi, R. Gomperts, R.L. Martin, D.J. Fox, T. Keith, M.A. Al-Laham, C.Y. Peng, A. Nanayakkara, M. Challacombe, P.M.W. Gill, B. Johnson, W. Chen, M.W. Wong, J.L. Andres, C. Gonzalez, M. Head-Gordon, E.S. Replogle, J.A. Pople, Gaussian Inc., Pittsburgh, PA, 1998.
[14] C. Glidwell, Inorg. Chim. Acta 20 (1976) 113.
[15] C. Glidwell, Inorg. Chim. Acta 36 (1979) 135.
[16] J.S. Wright, E.R. Johnson, G.A. DiLabio, J. Am. Chem. Soc. 123 (2001) 1173–1183.
[17] C.H. Schiesser, From Marco Polo to chiral stannanes—radical chemistry for the new millennium, Arkivoc, 2001.